






Cite this: DOI: 10.1039/d5ma00811e

## Quantifying fungal growth in 3D: an ergosterol-based method to distinguish growth modes

Natalie Nussbaum,  \* Laura Balmelli, Nadja Steiger, Laura Nyström, Peter Fischer  \* and Patrick A. Rühls 

Mycelium colonization of fungi on solid substrates occurs in three dimensions: hyphal extension on the substrate surface, mycelium network densification, and invasive hyphal growth into the substrate. Quantifying fungal biomass in three dimensions presents a challenge, because current methods either require the separation of mycelium from the host material or rely on pure 2D optical density measurements. Here, we quantitatively assessed fungal growth of *Ganoderma sessile* by measuring ergosterol, a sterol specific to fungi that effectively represents biomass estimation. To investigate and quantify the global fungal growth in 3D, we focused on two primary growth profiles: extensive growth, describing lateral colonization of hyphae across the substrate surface, and local growth, reflecting invasive penetration into the substrate and mycelium network densification. Distinguishing between these regimes is critical, as they contribute differently to biomass distribution and substrate interaction, enabling a more accurate and functionally relevant assessment of fungal growth in 3D systems. By measuring local and global ergosterol accumulation, we estimated that extensive growth contributes around 300 times more to global biomass accumulation than local growth. By altering the nutrient density and stiffness of the host materials, we assessed whether global biomass accumulation is primarily driven by extensive or local growth increase. Our results demonstrate that the common assumption that radial extension corresponds to biomass increase is not correct and consequently, not a reliable method for comparing fungal strains or growth conditions when interested in fungal biomass. Therefore, using ergosterol to measure the local and global growth allows the quantification of the contribution of both growth profiles to the final global biomass accumulation, providing an approach that can quantify the effects of substrate morphology and nutrient density.

Received 26th July 2025,  
Accepted 1st September 2025

DOI: 10.1039/d5ma00811e

[rsc.li/materials-advances](https://rsc.li/materials-advances)

## Introduction

Fungal mycelium has emerged as a novel material with unique properties, attracting interest for its potential in creating biomaterials<sup>1–5</sup> and engineered living materials.<sup>6–9</sup> A significant challenge is the quantitative assessment of mycelium biomass in three-dimensional (3D) substrates, where separating the mycelium from the host material can be difficult. Current approaches to measure fungal growth, such as optical density or microscopy techniques, are limited in their ability to capture 3D growth patterns and biomass distribution. Ergosterol quantification offers a precise and spatially resolved alternative, enabling accurate estimation of fungal biomass in solid-state systems. Developing reliable 3D biomass measurement approaches is therefore crucial for advancing the applications of mycelium in various fields. Beyond bio-based leathers and engineered living systems, fungal mycelium is increasingly studied for its use in packaging

and insulation materials,<sup>10,11</sup> construction composites,<sup>1,12,13</sup> and even biomedical scaffolds.<sup>2,14</sup> These diverse applications highlight the need for reliable biomass quantification methods, as precise measurement is essential for optimizing growth conditions, ensuring reproducibility, and tailoring material properties to meet practical requirements.

The fungal biomass assessment methods in solid-state fermentation (SSF) can be classified into indirect and direct approaches. Indirect methods—such as radial growth assessment, optical density (OD) analysis, and image processing—are time-efficient but lack precision. Radial growth measurement is a simple approach for tracking fungal colony extension by periodically measuring its diameter.<sup>15,16</sup> However, this method only captures the growth of aerial hyphae and does not account for colony density or biomass accumulation within the substrate. In addition, this method is limited to 2D fungal growth on culture plates.

Optical density measurements offer another way to estimate fungal biomass by assessing the culture's absorbance. This technique is easy to perform, cost-effective, and requires

ETH Zürich, IFNH, 8092 Zürich, Switzerland.  
E-mail: [natalie.nussbaum@hest.ethz.ch](mailto:natalie.nussbaum@hest.ethz.ch), [peter.fischer@hest.ethz.ch](mailto:peter.fischer@hest.ethz.ch)



minimal specialized equipment.<sup>17,18</sup> However, its accuracy can be influenced by factors such as fungal metabolites and culture pigmentation, potentially leading to measurement inconsistencies.<sup>19</sup> Similarly, image analysis provides a rapid and non-destructive means of monitoring fungal growth.<sup>20,21</sup> While effective, this method demands specialized software, technical expertise, and careful standardization to ensure reliable results.

In contrast, direct methods, which include dry weight measurement, protein content analysis, and ergosterol extraction, provide better accuracy. Among direct methods, dry weight measurement is one of the simplest ways to quantify mycelial biomass, involving the drying and weighing of mycelium after growth. However, this approach requires isolating the mycelium from its substrate, making it impractical when the mycelium is embedded within the substrate, such as in scaffold-based growth.<sup>22,23</sup> Protein content analysis relies on techniques such as the Bradford or Lowry Assay and correlates with biomass.<sup>24</sup> However, this method is unsuitable when the substrate itself contains protein, as it can interfere with accurate measurements.<sup>25</sup> While these methods are effective for strain screening and quick proof-of-concept studies, a precise quantification technique is still necessary for accurately measuring fungal growth in solid substrates. In addition, methods capable of distinguishing fungal growth modes are increasingly needed, since surface-associated expansion and local growth have very different implications for both ecological functioning and material applications.<sup>9,26,27</sup>

Current quantification techniques often overlook this distinction, limiting their ability to fully capture fungal developmental strategies and performance in applied contexts.

Recent advances have introduced cutting-edge 3D quantification alternatives, including high-resolution microscopy techniques<sup>28–31</sup> and biosensor-based systems,<sup>32,33</sup> which enable spatially resolved and dynamic monitoring of fungal biomass. While these emerging methods hold promise for future applications, they are often costly, technically demanding, and not yet widely accessible. Therefore, another robust and accessible technique is still necessary to overcome these limitations and provide reliable quantification of fungal growth in solid-state systems.

This challenge can be addressed by quantifying ergosterol to assess fungal biomass. Ergosterol is a sterol found exclusively in fungal cell walls<sup>34</sup> and is an established standard for determining metabolically active biomass, as it is remarkably stable when protected from light.<sup>35,36</sup> It can be extracted from fungal samples and quantified using high-performance liquid chromatography (HPLC). Ergosterol is typically expressed as the amount of ergosterol per unit weight of the analyzed sample or as the total yield relative to the substrate weight.<sup>37–40</sup> Pure fungal mycelium can also be analyzed to determine conversion factors that relate the ergosterol content directly to fungal biomass.<sup>36,41,42</sup> Although this method is precise and widely considered a standard in the field, protocols are time-consuming.<sup>38,39,43,44</sup> Additionally, there is limited research on the suitability of using this method to quantify mycelial growth

over time or distinguish between directions of growth within solid substrate host materials.

Here, we employed an efficient protocol for the extraction of ergosterol and compared the quantified values with the standard radial growth method. In the first section, we analyzed fungal growth on a substrate agar plate to demonstrate the correlation between ergosterol levels and fungal growth over time. We further focused on ergosterol accumulation by examining three-dimensional growth profiles: hyphal extension along the *x*-plane (extensive growth) and local growth, which encompasses both invasive penetration along the *z*-plane of the substrate and densification of the mycelial network. Here, we use the term local growth consistently to describe these two processes, distinguishing it from extensive growth. To validate the suitability of ergosterol quantification for measuring fungal growth, we evaluated how modifications to the substrate impact mycelial growth in the subsequent sections. With the quantification method at hand, our focus was on the key growth factors in the substrate that influence fungal proliferation. Specifically, in the second section, we examined malt concentration as the primary carbon source in the solid substrate, and in the third section, we addressed agar concentration, which affects the gel strength<sup>45</sup> of the solid substrate. This approach allows us to assess how alterations in the host material affect global ergosterol accumulation and differentiate between extensive and local growth. Unlike prior ergosterol-based assays developed primarily in the context of soil microbiology,<sup>38,43</sup> where the method is typically applied to estimate fungal biomass in heterogeneous and microbially diverse systems, our approach adapts and extends ergosterol quantification to controlled, solid-state substrates. This adaptation enables spatially resolved insights into fungal growth dynamics and, crucially, the differentiation between extensive and local growth modes. By establishing this methodological bridge, we position ergosterol quantification as a suited tool for investigating fungal behavior in materials science, tissue engineering, and mycelium-based composite applications.

## Materials and methods

### Materials

All materials and equipment used for fungal cultivation were prepared in a sterile environment in a SafeFAST Premium 215 bench (Faster, Italy). This study was conducted using two fungal strains: *Ganoderma sessile* species (code 95-19, MOGU S.r.l, Italy) and *Ganoderma lucidum* (code MG11500, Mycogenetics, Germany) from the Basidiomycetes family. All raw materials for the growth substrate were received as powders. Malt extract and agar were received from Morga AG (Switzerland), and yeast extract was received from Thermo Fisher Scientific (Germany). For the ergosterol extraction, HPLC-grade methanol ( $\geq 99.9\%$ ), HPLC-grade chloroform ( $\geq 99.9\%$ ), ergosterol standard (certified reference material) and cholesterol standard (certified reference material) were sourced from Sigma Aldrich (Germany).



## Methods

### Maintenance of fungal cultures and media preparation.

Cultures were maintained in vented 90 mm-diameter Petri dishes (VWR, USA), sealed with Parafilm (Bemis Company Inc., USA). They were incubated in the dark at 30 °C on a defined standard malt agar substrate (SMA), containing 2 wt% malt extract (ME), 2 wt% agar, and 0.2 wt% yeast extract and transferred to a new plate weekly. For substrate modifications, the agar concentration in the SMA substrate was adjusted from 2 wt% to 0.5–4 wt% without changing the malt or yeast extract concentrations. Similarly, malt extract concentrations were varied from 2 wt% to 0.25–20 wt%. All incubation events were run in the dark at 30 °C and 80% relative humidity. For all experiments, the inoculum was consistently taken from the edge of a max. 5-Day-old radial fungal colony grown on agar to ensure the use of fresh and active culture material.

**Growth kinetics.** The mycelium extension was traced daily until plates were fully colonized (6–7 days). Petri dishes were inoculated in the middle with 5 mm diameter discs of mycelium from the edge of 3 to 5 day old growing colonies. For each day of growth, extension was measured radially from the point of inoculation, taking 4 measurements per day over a cross drawn on the plate. The radial extension in cm was plotted against time in days, and a linear fit was applied to determine the slope, representing the radial extension rate in  $\text{cm day}^{-1}$ . The growth area was calculated daily by determining the area of the newly formed circle based on the measured radius. For each condition, 3 biological replicates were considered.

**Rheology.** Rheological measurements were done with an MCR 702 Twin Drive Rheometer (Anton Paar) with a rough plate geometry (PP25/S) of 25 mm. For the test, 4 mm thick and 20 mm diameter discs of gelled solid substrates were cut and placed on a tempered geometry. The temperature was maintained at a constant 30 °C using a Peltier bottom geometry, chosen to match the conditions inside the incubator where the mycelium was cultivated. Initially, a frequency sweep was carried out at 0.1% strain, spanning from 100 to 0.1  $\text{rad s}^{-1}$ . Subsequently, an amplitude sweep was conducted at 1  $\text{rad s}^{-1}$ , ranging from 0.01 to 100% strain, to confirm 0.1% strain lies within the linear viscoelastic region.

**Fungal biomass quantification via ergosterol extraction.** To monitor ergosterol levels throughout the incubation period, entire Petri dishes were processed for extraction, except in the experiments involving local ergosterol via age rings (see next section). We can assume that the substrate itself contained no detectable amounts of ergosterol, as indicated by the absence of peaks in control samples, as shown in SI Fig. S1. After cultivation, the mycelium samples were freeze-dried using a FreeZone 4.5L Benchtop Freeze Dryer (Labconco, USA) and then ground into homogenized powders. Ergosterol was extracted using a modified method based on Alekseyeva *et al.*<sup>44</sup> This extraction process involved methanol and chloroform as solvents. To isolate the total lipid fraction, we applied the standardized lipid extraction method by Bligh and Dyer.<sup>46</sup> The total weight of the freeze-dried substrate-mycelium mix for each sample was recorded and 300 mg of this mix was weighed into

30 ml Pyrex tubes. The tubes were wrapped in foil to protect them from UV rays and prevent potential degradation of ergosterol. To each sample, 1 ml of an internal standard solution (2  $\text{mg ml}^{-1}$  cholesterol in 95 : 5 chloroform–methanol) and 9 ml of a 2 : 1 chloroform–methanol solvent were added. The samples were then vortexed and sonicated for 20 minutes at room temperature. Following this, 4 ml of Milli-Q water was added to each sample, and the mixture was vortexed and sonicated for another 20 minutes. The samples were then centrifuged at 1000g for 3 minutes using a 5810 R centrifuge (Eppendorf, Germany). After centrifugation, clear phase separation was observed. Sterols were extracted by transferring the lower phase into clean vials using a glass pipette. A second washing step was performed by adding 9 ml of chloroform to the original vials, mixing, centrifuging, and again transferring the lower phase to the clean vials. The solvent in the vials was evaporated under a nitrogen stream at 40 °C. After evaporation, 1 ml of a 95 : 5 chloroform–methanol solvent was added to redissolve the cholesterol and ergosterol. The extraction efficiency of various chloroform–methanol ratios was previously tested and is detailed in SI Fig. S2. The samples were sonicated at room temperature for 20 minutes to ensure complete dissolution, which was verified optically. Finally, the samples were filtered through 0.45  $\mu\text{m}$  nylon filters and transferred to amber HPLC vials for subsequent analysis. The samples were analyzed using high-performance liquid chromatography (HPLC) with an Agilent 1200 series system (Agilent Technologies, USA) equipped with a Nucleodur C 18 ec column (Macherey-Nagel, Germany) and quantified using the Chromeleon software (Chromeleon 7.2.7, Thermo Scientific, USA). Cholesterol and ergosterol concentrations were determined by integrating the peaks measured via HPLC at specific wavelengths: 205 nm for cholesterol<sup>47,48</sup> and 282 nm for ergosterol.<sup>38,44</sup> The ergosterol concentration in each sample was quantified by adjusting the measured values based on the recovery of the internal standard in each sample, as well as the total weight of the sample. The quality of the extraction was confirmed, with the internal standard recovery being over 87% for all samples. All measurements were performed within the assay's working range, and an ergosterol standard calibration series covering the full range of observed concentrations was included in each experiment to ensure accurate and reliable quantification.

**Local ergosterol via age rings.** To quantify local ergosterol content, we relied on the growth pattern of radial mycelium growth on a Petri dish. Since mycelium grows radially on a Petri dish, we could take advantage of this pattern by marking the inoculation point and drawing a cross on the substrate as a reference. From this point, we traced daily age rings corresponding to each day of radial growth. This approach allowed us to later separate the sample into distinct daily age segments at the end of the incubation period. A schematic overview of how the Petri dish samples were cut into age rings is shown in Fig. S6 SI.

It should be noted that the daily marking of fungal growth rings does not aim to represent distinct growth phases, but merely allow to estimate the impact of average mycelium age on



ergosterol content. Also, environmental fluctuations (*e.g.*, temperature or humidity changes) may also affect growth rates, causing minor deviations in the daily marked distances. Despite these limitations, the Petri dish model allows sufficiently uniform radial growth to make daily ring separation a practical approach for evaluating the relationship between mycelium age and ergosterol accumulation.

**Descriptive statistics.** To compare the mean ergosterol levels between two conditions, a one-way ANOVA followed by Tukey's *post hoc* test was performed. Prior to the analysis, the homogeneity of variances was confirmed with a Levene's test of equal variances. In the figures presented, asterisks (\*) are used to indicate levels of statistical significance and *p*-values are reported as follows:  $p < 0.05$  (\*),  $p < 0.01$  (\*\*) and  $p < 0.001$  (\*\*\*). The statistical analysis was performed using Origin Pro 2021 9.8.0.200 software (OriginLab Corporation, Northampton, MA, USA).

## Results and discussion

### Mycelial growth over time

To quantify fungal biomass over time, we employed ergosterol analysis, a well-established method that correlates with the amount of mycelial material.<sup>38,44,49</sup> Our results support that ergosterol analysis is a good measure to quantify fungal mycelium biomass (Fig. 1). We investigated the biomass of filamentous fungi grown on a standard solid substrate (2 wt% malt extract, 2 wt% agar and 0.2 wt% yeast extract) *via* ergosterol quantification and compared it to extensive fungal growth along the host materials's surface (*x*-direction) *via* radial growth measurements. After establishing a linear correlation between ergosterol and dry mycelium biomass for two *Ganoderma* strains (see SI Fig. S3), we evaluated the suitability of ergosterol quantification as an indicator of fungal growth over time. Ergosterol is a sterol found only in fungal cells, and its amount increases as the fungus grows.<sup>40,44</sup> Therefore, measuring

ergosterol provides a time-resolved indication of fungal growth dynamics, complementing the spatial information obtained from radial growth measurements.

The global ergosterol content was quantified per single mycelial culture on solid substrate in a Petri dish, accounting for both aerial and substrate-bound mycelium. A logistic correlation for *G. sessile* was observed (Fig. 1a) by fitting the model described in eqn (1) ( $R^2 = 0.99$ ):

$$E = \frac{E_2 + (E_1 - E_2)}{1 + (t/t_i)^p} \quad (1)$$

where  $E$  is the ergosterol content at time  $t$ ,  $E_1$  the initial ergosterol content,  $E_2$  the final value of ergosterol content,  $t_i$  the inflection point and  $p$  the shape parameter. A logistic model features slow initial growth that accelerates rapidly, but as it approaches the carrying capacity ( $E_2$ ), growth slows and levels off, creating an S-shaped curve. The inflection point marks the highest growth rate.<sup>50,51</sup> The logistic model for *G. sessile* is an appropriate fit because it reflects the limited growth conditions in our system, where both substrate and space (Petri dish) impose natural constraints on the population. The inflection point  $t_i$  is about 5.5 d, marked with a star symbol in Fig. 1a. It describes the point where growth transitions from an exponential to a stationary phase. Measuring the radial extension of *G. sessile*, the Petri dish was fully covered at day 6, hence the mycelial colony reached the edge of the dish between day 5 and 6, which is perfectly reflected in the inflection point at the time point 5.5 days. The logistic growth model is commonly used in literature to describe fungal growth.<sup>24,37,52–54</sup> The exponential growth phase was also observed in the relationship of ergosterol over time for another *Ganoderma* strain, as shown in SI Fig. S4. The details of the fitting parameters are not discussed further, as the fits primarily serve to illustrate that the accumulation of ergosterol over time follows a plausible model for *Ganoderma* spp. To directly compare the biomass quantified with radial growth analysis, we measured the growth area,

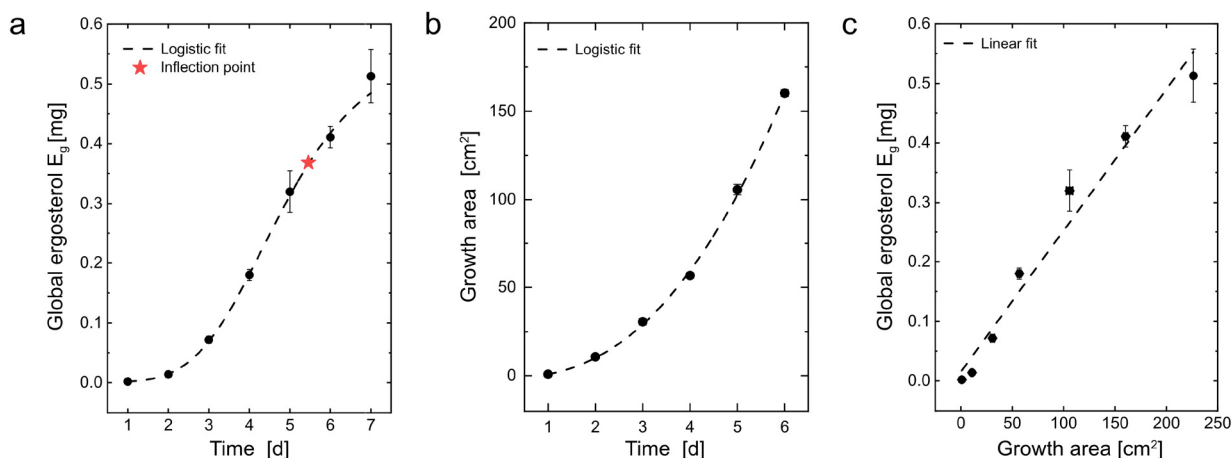


**Fig. 1** (a) Global ergosterol over time. The inflection point observed from the regression analysis indicates a shift in the growth dynamics, corresponding to a slowdown in ergosterol accumulation. (b) Mycelium growth area calculated from radial extension over time. Data points are shown only up to day 6, as the colony had reached the edge of the Petri dish thereafter. (c) Linear correlation between global ergosterol values shown in (a) and the mycelium growth area plotted in (b). All data correspond to mycelium from *G. sessile*  $n = 4$  for all data.



which represents the mycelial mat that forms over time (Fig. 1b). This was calculated from assessing radial extension (see SI Fig. S5). The ergosterol levels and growth area of *G. sessile* were fitted to a linear regression, yielding a slope of  $2.4 \times 10^{-3} \pm 1.8 \times 10^{-4}$  ( $R^2$ -value = 0.97) (Fig. 1c). For each  $\text{cm}^2$  of mycelial mat growth, the ergosterol content increases by  $2.4 \times 10^{-3}$  mg. The linear correlation indicates that the measurement of the growth area, which only accounts for two-dimensional fungal growth, is closely correlated with the totally accumulated biomass (*i.e.* three-dimensional) of *G. sessile* on the studied substrate. A linear correlation between fungal growth and ergosterol quantified has previously been reported in a study by Montgomery *et al.*,<sup>38</sup> where the total fungal dry biomass correlated linearly with total ergosterol. Similarly, ergosterol concentration was linearly related to fungal biomass by Alekseyeva *et al.*<sup>44</sup>

### From global to extensive and local growth

As the ergosterol content of *G. sessile* follows a typical evolution over time, it can be considered a realistic measure for fungal biomass in our samples. While we have established the suitability of quantifying total fungal biomass accumulation *via*

ergosterol, this section introduces a new idea: to distinguish the global accumulation of biomass in different directions of 3D growth. Specifically, differentiating between fungal growth in the *x*-direction (extensive) *versus* invasive growth in the *z*-direction and mycelium density increase (local). A schematic explaining the terminology used to describe the fungal growth in different directions within the host material is shown in Fig. 2.

The global biomass accumulation on a standard substrate (2 wt% ME, 2 wt% agar and 0.2 wt% yeast extract) likely accumulates more from extensive growth in the *x*-direction, with less contribution from local growth through increased branching, metabolic changes and invasive hyphal growth into the substrate (Fig. 3). We studied the local mycelial growth over time by quantifying the ergosterol content per sample fragment ( $\text{mg mg}^{-1}$ ) at different ages of the mycelium culture. This reflects how mycelial biomass accumulates over time in place (local growth) without including mycelial extension in the *z*-direction.

The ergosterol content per mg of sample increases with culture age (Fig. 3a). For example, a 1-day-old culture corresponds to  $1.4 \times 10^{-3}$  mg ergosterol per mg sample, while a

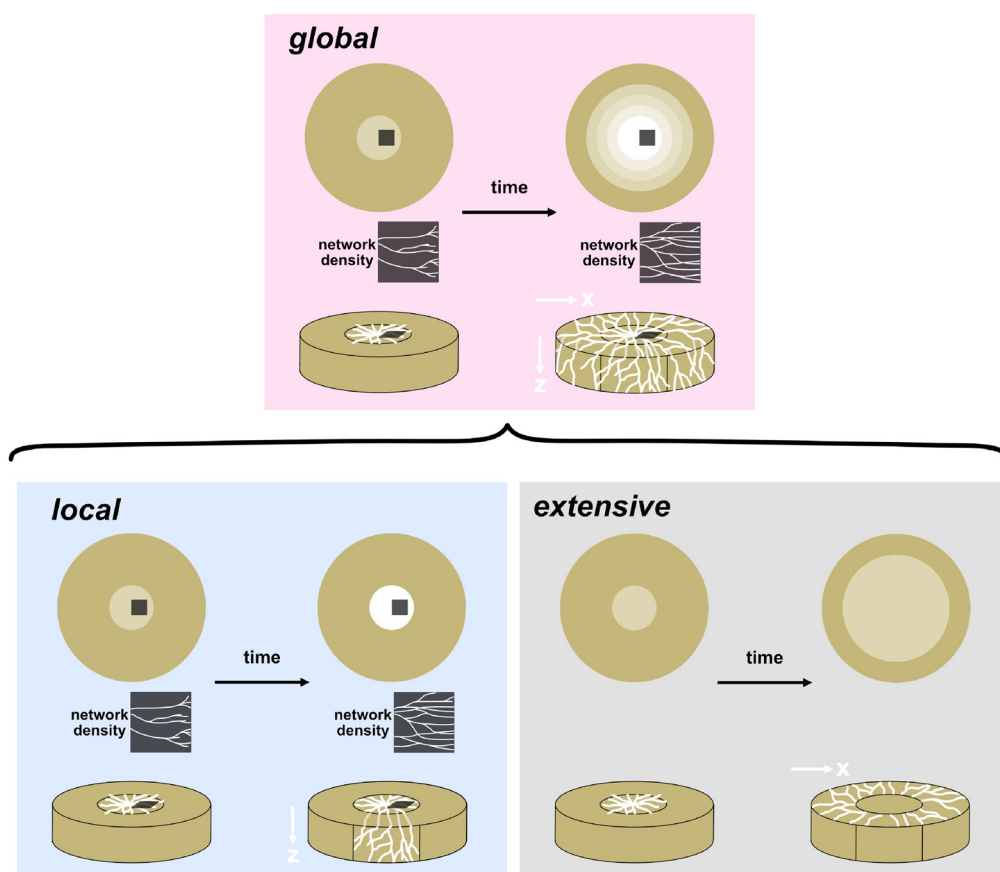


**Fig. 2** A schematic illustrating the fungal growth in different directions within its host material: local growth, describing fungal growth in the *z*-direction of the host material and including branching patterns; extensive growth, only taking into account the mycelium extension in the *x*-direction; and global growth, a combination of both local growth and extensive growth, with mycelium expanding in the *x*-direction and growing in the *z*-direction and branching patterns across the surface. The diagram schematically represents each growth profile, emphasizing the distinct directional and branching behaviors of mycelium in each case.



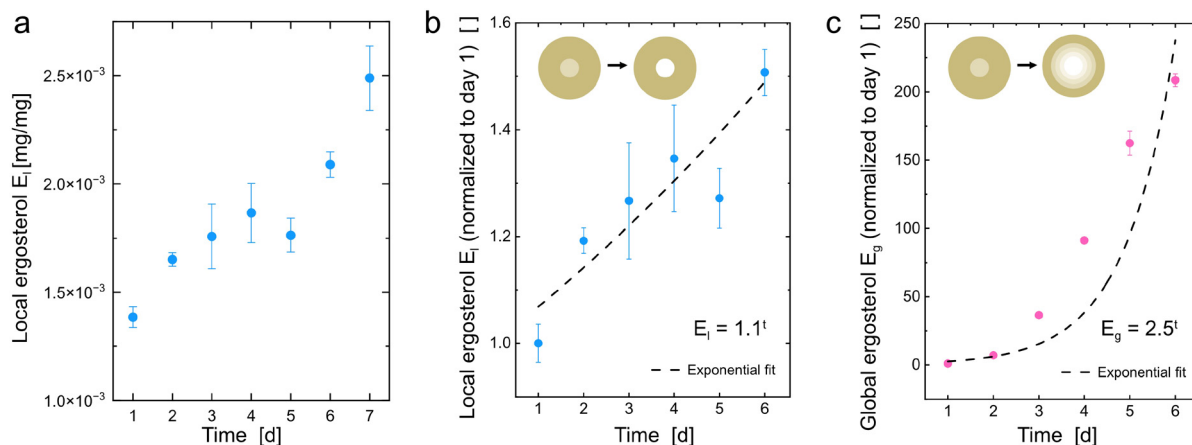


Fig. 3 (a) Local ergosterol per mg of substrate quantified over time for different mycelium culture ages. (b) Local ergosterol normalized to day 1 (reference factor = 1) and shown over time. (c) Global ergosterol normalized to day 1 (reference factor = 1) and shown over time. All ergosterol data correspond to mycelium from *G. sessile*  $n = 4$  for all data.

7-day-old culture corresponds to  $2.5 \times 10^{-3}$  mg ergosterol per mg sample, representing an increase of nearly 80%. Fig. S6 SI presents a schematic overview of how the samples were prepared to quantify local ergosterol contents shown in Fig. 3a. Since mycelium grows radially, we could mark age rings daily, allowing the sample to be separated into distinct daily age segments at the end of the incubation. In contrast, the data presented in Fig. 1a represents global fungal growth, capturing the total increase in ergosterol through branching, metabolic changes, invasive growth in the  $z$ -direction and extension in the  $x$ -direction. In Fig. 3b the increase of ergosterol in place over time (local growth) is shown relative to day 1, which is set as a reference factor of 1. The  $y$ -axis represents the fold increase in ergosterol content compared to day 1. The data could be fitted with a power law ( $R^2 = 0.84$ )

$$E_l = 1.1^t \quad (2)$$

where  $E_l$  represents the local ergosterol content at time  $t$  relative to day 1. Similarly, Fig. 3c represents the increase of global ergosterol content over time, derived from the data in Fig. 1a, normalized to day 1. This data could also be fitted with a power law ( $R^2 = 0.78$ )

$$E_g = 2.5^t \quad (3)$$

with  $E_g$  as the global ergosterol content at time  $t$  relative to day 1. Thus, if we assume that  $E_g \triangleq E_l + E_e$  we can quantify how much more the extensive growth  $E_e$  contributes to  $E_g$  compared to the local growth  $E_l$  by comparing the relative rates of increase between the two.

$$\frac{E_e}{E_l} = \frac{2.5^t - 1.1^t}{1.1^t} \quad (4)$$

Thus, at  $t = 1$ , extensive growth contributes about 1.27 times more to global ergosterol than local growth does, whereas at  $t = 7$ , its contribution is about 300 times larger.

To date, there has been no research highlighting the influence of the mycelium culture age on the total ergosterol content

of a fungal sample. Our findings address this gap and enhance understanding of fungal growth dynamics within the 3D environment of solid-state fermentation. The differences in local ergosterol over time may arise from various factors. One key factor is culture age, as lower ergosterol levels have been observed in aging mycelium compared to freshly grown cultures due to increased stress and downregulation of ergosterol biosynthesis.<sup>55</sup> Another factor is the change in mycelium network density, since the branching frequency tends to increase in older mycelium near the inoculum, where growth has been established for longer.<sup>56</sup> Further, the thickness of the mycelium mat directly affects the biomass per milligram of sample. As mycelium colonizes a (semi-)solid substrate, it initially spreads across the surface to efficiently utilize nutrients and oxygen. Depending on the stiffness of the substrate, invasive growth occurs at a later stage.<sup>45,57</sup> Thus, we can assume that the older mycelium develops a thicker mat along the  $z$ -plane due to deeper invasion into the substrate.

While our study distinguishes between global and local growth, it does not directly address how these growth regimes influence the physical properties of the mycelial biomass, such as porosity, density or mechanical strength. These aspects are highly relevant for applications where the material function of mycelium is critical (*e.g.*, construction composites, packaging, and engineered living materials). We see our method as a first step toward enabling such investigations, however, future studies integrating ergosterol quantification with material characterization techniques will be necessary to establish these connections. We would like to note that the age ring method provides insight into how mycelium age affects biomass accumulation but relies on uniform radial growth on Petri dishes. In heterogeneous 3D substrates, age-specific biomass cannot be reliably separated, so our results serve as a proof-of-concept under controlled conditions, with further work needed for more complex systems. Our findings can be summarized as follows. We demonstrated that the relative ergosterol content per mg of sample, both locally (in place) and globally (across



the whole sample) increases over time by following power laws. Further, we can conclude that for a host material composed of 2 wt% ME, 2 wt% agar, 0.2 wt% YE and water, the local growth constitutes a minor portion of the global growth, with the majority potentially coming from extensive fungal growth. Now that we know ergosterol is a reliable measure for fungal biomass, we aim to confirm if this remains valid when modifying the host material composition.

### Effect of host material malt extract concentration on mycelial growth

Increasing the malt extract (ME) concentration in the host material decreases the extensive (2D) growth of mycelium (x-plane of the Petri dish) but increases the global biomass, or 3D fungal growth (Fig. 4). The effect of various malt extract concentrations in the host material was studied *via* radial extension and biomass quantification. As the malt extract concentration in the substrate increases from 0.5 to 20 wt%, the 2D extension of mycelium decreases linearly ( $R^2 = 0.98$ ), with a reduction of  $0.05 \text{ cm day}^{-1}$  for each additional wt% of ME in the substrate (Fig. 4a). The radial extension was determined from the slope of radial growth curves over time (SI Fig. S5a).

Fig. 4b shows the quantified global ergosterol of mycelium grown on host materials with different malt concentrations over the incubation time. The data suggests an increase in ergosterol levels with increasing malt extract concentration and after 7 days, ergosterol for 8 wt% ME substrate is significantly higher than for 2 and 1 wt% ME substrate (statistical details are provided in the ANOVA table in SI Table S1). Fig. 4c illustrates the global ergosterol content in mg in the mycelium cultivated for 7 days at the different concentrations of ME in the substrate in wt%. In contrast to the trend observed for extensive growth, the global fungal biomass increases with increasing ME concentration in the substrate. As the ME concentration increases from 1 to 8 wt%, the ergosterol quantity increases linearly with a slope of  $0.041 \text{ mg}$  for each additional wt% of ME in the substrate ( $R^2 = 0.98$ ). The increase in mycelium growth area follows an exponential trend over time for all tested substrates (Fig. 4d), consistent with the growth curve observed for the 2 wt% malt substrate shown in Fig. 1b. To compare the mycelium growth area and global ergosterol accumulation over time, the data was correlated and fitted using linear regression in Fig. 4e (fit details in SI Table S2), supporting the results shown in Fig. 1c. Namely, that fungal growth quantified by both

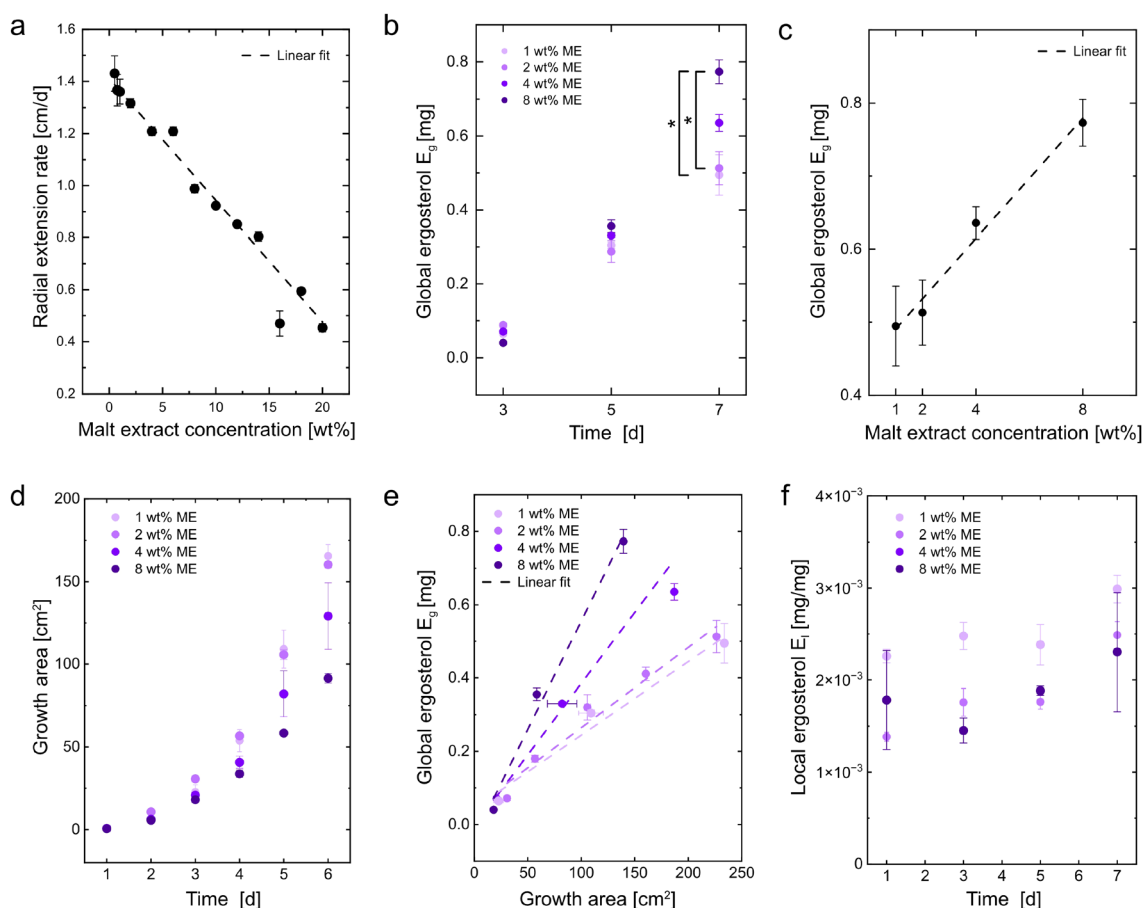


**Fig. 4** (a) Radial extension of mycelium as a function of varying malt concentrations in the substrate. (b) Change in global ergosterol over time,  $p$ -Values: 1 wt% ME vs. 8 wt% ME,  $p = 0.002$ ; 2 wt% ME vs. 8 wt% ME,  $p = 0.003$  (c) correlation between global ergosterol and malt concentration in the substrate. (d) Radial extension over time, represented as growth area. (e) Correlation between global ergosterol and growth area. (f) Change in local ergosterol over time. All data correspond to mycelium from *G. sessile*  $n = 4$  for all data.



growth area and global ergosterol follow a proportional relationship over time.

Fig. 4f shows the ergosterol content from local growth analysis across different substrates. No significant change in local growth patterns relative to ME concentration was observed. However, recent studies indicate that fungal growth on nutrient-rich substrates leads to increased mycelium network density,<sup>17,18</sup> which offers one explanation for the rise in global ergosterol with increasing ME concentration in the substrate.

When comparing the 8 wt% ME substrate to the standard 2 wt% ME substrate, we observed a 34% reduction in extensive growth (average extension  $\bar{x} = 0.98 \text{ cm day}^{-1}$  for the 8 wt% substrate vs.  $1.31 \text{ cm day}^{-1}$  for the 2 wt% substrate). Additionally, there was a 34% increase in global ergosterol levels (average value  $\bar{x} = 0.77 \text{ mg}$  after 7 days for the 8 wt% ME substrate vs.  $0.51 \text{ mg}$  for the 2 wt% substrate).

Previous research has shown that when sugars in the solid substrate are more readily available, there is an increase in metabolite production, an increase in hyphal extension and greater biomass production.<sup>17,58</sup> This finding is consistent with earlier research on *G. sessile*, which found that higher malt concentrations in the substrate resulted in increased stiffness

and network density.<sup>18</sup> While our study focused on how nutrient density affects overall biomass accumulation, we did not specifically investigate how these conditions influence distinct stages of mycelial development. This could be addressed in future work to further understand the relationship between substrate composition and fungal development.

Based on our results, we can draw two key conclusions about the effect of malt extract concentration on mycelial growth. First, as the malt extract (ME) concentration increases, the radial extension (2D) of the mycelium decreases. Second, in contrast to the radial extension, the total biomass (3D), which represents global mycelial growth, increases with higher malt content in the substrate. This is consistent with our previous study, where higher wt% of ME in the substrate slowed radial growth of *G. sessile* compared to the 2 wt% ME substrate.<sup>18</sup> Similarly, Gantenbein *et al.*<sup>5</sup> observed that radial extension peaked at 2 wt% ME and slowed with increasing ME concentrations.

Thus, when the nutrient availability in the substrate is increased, global biomass accumulation is not driven by radial extension, but rather local growth patterns or metabolic changes in ergosterol biosynthesis. In addition to malt extract

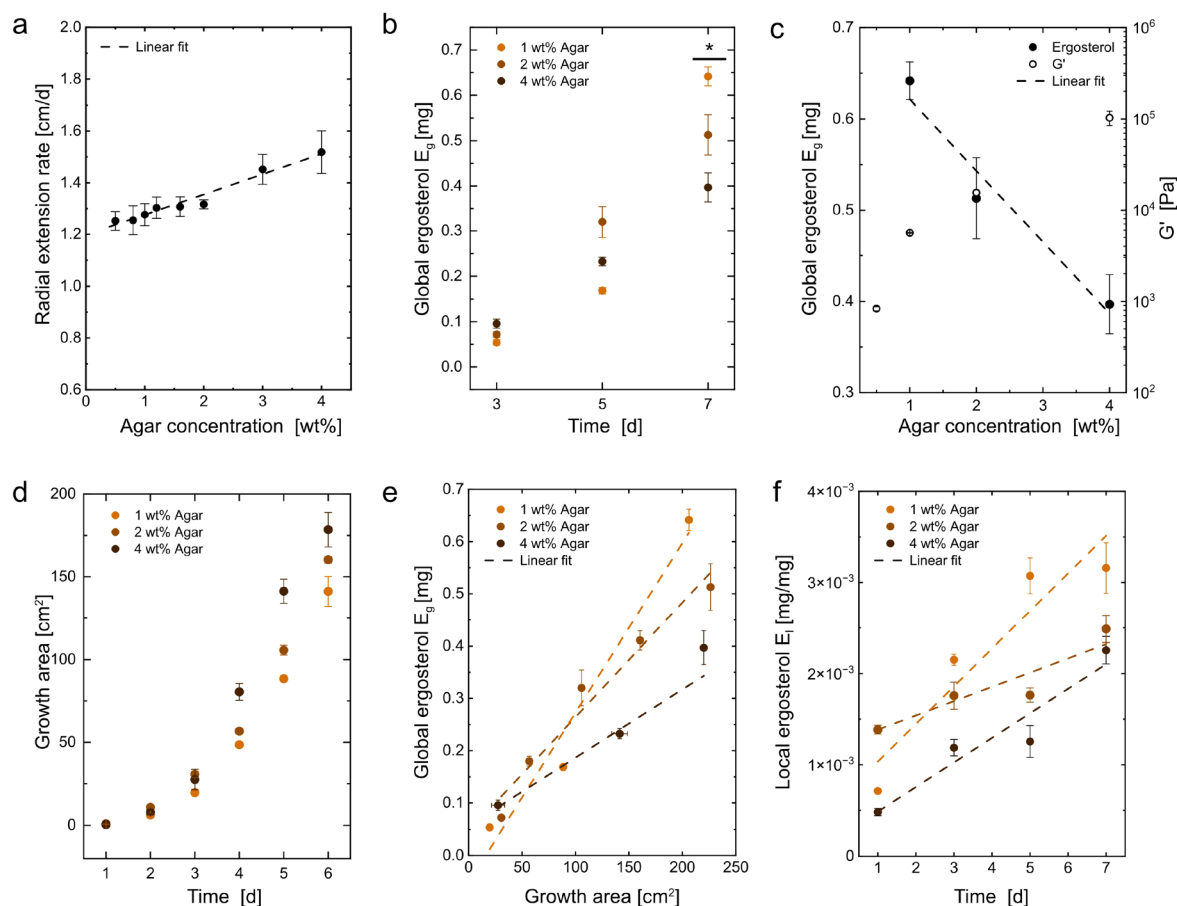


**Fig. 5** (a) Radial extension of mycelium as a function of varying agar concentrations in the substrate. (b) Change in global ergosterol over time.  $p$ -Values: 1 wt% Agar vs. 2 wt% Agar,  $p = 0.011$ ; 1 wt% ME vs. 4 wt% ME,  $p = 1.6 \times 10^{-4}$ ; 2 wt% Agar vs. 4 wt% Agar,  $p = 0.026$  (c) correlation between global ergosterol, agar concentration and  $G'$  of the substrate. (d) Radial extension over time, represented as growth area. (e) Correlation between global ergosterol and growth area. (f) Change in local ergosterol over time. All data correspond to mycelium from *G. sessile*  $n = 4$  for all data.



concentration, the agar concentration of the solid substrate may also influence the 3D growth of mycelium. In the following section, we will examine the impact of the stiffness of the host material on fungal growth patterns.

### Effect of host material stiffness on fungal growth

Extensive fungal growth increases linearly with the stiffness of the host material, while global biomass accumulation is highest in the softest material (1 wt%) compared to both 2 and 4 wt% agar (Fig. 5). Similar to malt extract concentration, the impact of various concentrations of agar in the substrate on fungal growth was studied *via* radial extension and biomass quantification. As the agar concentration in the substrate increases from 0.5 to 4 wt%, the extensive mycelial growth follows a linear trend ( $R^2 = 0.96$ ), increasing by  $0.079 \text{ cm day}^{-1}$  for each additional wt% of agar in the substrate (Fig. 5a). The radial extension was determined from the slope of radial growth curves over time (SI Fig. S5b). Fig. 5b displays the global quantified ergosterol in mycelium cultivated on substrates with varying agar concentrations at different incubation times. The ergosterol accumulation over time likely follow a logistic trend, with significantly higher ergosterol contents after 7 days in 1 wt% agar compared to 2 and 4 wt% agar ( $p < 0.05$ , see details in ANOVA table in SI Table S1). Fig. 5c illustrates the correlation between ergosterol in mycelium cultivated for 7 days on substrates with varying agar concentrations, and gel strength, determined as  $G'$  values in the linear viscoelastic (LVE) region of amplitude sweeps of the agar gels. The corresponding rheological data is shown in Fig. S7 SI.  $G'$  increases with higher agar concentrations, consistent with findings reported in the literature,<sup>9,45,59</sup> while the global ergosterol levels decrease with increasing agar concentration in the substrate. As the agar concentration increases from 1 to 4 wt%, the global ergosterol decreases linearly with a slope of  $-0.078 \text{ mg}$  for each additional wt% of agar in the substrate ( $R^2 = 0.90$ ). The relationship between ergosterol and  $G'$  follows a power-law decay and is presented in Fig. S8 SI. The radial extension shown as mycelium growth area over time follows an exponential trend for all tested host materials (Fig. 5d), consistent with previous data showing the evolution of mycelium growth area of *G. sessile* over time. The mycelium growth area over time was again directly compared to the global ergosterol accumulation over time, shown in Fig. 5e. The data can be fitted using linear regression (fit details in SI Table S2), further supporting previous results from Fig. 1c and 4e. Fig. 5f shows ergosterol from local growth analysis across different agar substrates. Over time, the ergosterol per substrate in  $\text{mg mg}^{-1}$  increases the most in the lower agar concentration (1 wt%) substrate with  $4.1 \times 10^{-4} \text{ mg mg}^{-1} \text{ d}^{-1}$  ( $R^2 = 0.82$ ). In contrast, the trends are more gradual for the stiffer substrates, with  $1.6 \times 10^{-4} \text{ mg mg}^{-1} \text{ d}^{-1}$  for 2 wt% ( $R^2 = 0.84$ ) and  $2.7 \times 10^{-4} \text{ mg mg}^{-1} \text{ d}^{-1}$  for 4 wt% ( $R^2 = 0.86$ ).

We observed a 25% increase in global ergosterol in the softer substrate (1 wt%) compared to the standard 2 wt% agar substrate after 7 days of growth (average  $\bar{x} = 0.64$  vs.  $0.51 \text{ mg}$ ). The softer 1 wt% agar substrate showed 3% slower extensive growth compared to 2 wt% agar substrate (average  $\bar{x} = 1.27$  vs.

$1.31 \text{ cm day}^{-1}$ ), yet its local ergosterol content was 150% higher (average  $\bar{x} = 5.68 \times 10^{-4}$  vs.  $2.31 \times 10^{-4} \text{ mg mg}^{-1}$ ). The higher local ergosterol accumulation thus most likely resulted in the higher global ergosterol content for the softer substrate. Conversely, for the 4 wt% substrate, while extensive growth was faster than at 2 wt%, the global ergosterol levels were lower.

A recent study by Yang *et al.*<sup>60</sup> demonstrated that the mycelial growth of *Ganoderma lucidum* and *Pleurotus eryngii* was influenced by substrate stiffness. Agar concentrations of 1–4.5 wt% were investigated, with faster radial extension observed on stiffer substrates, which aligns with our findings. Softer substrates promoted mycelial growth into the three-dimensional space of the substrate but limited surface growth. Further, a study by Hotz *et al.*<sup>61</sup> showed that by increasing the agar concentration from 1.5 to 6 wt%, the mycelium density and hyphal width increased linearly. Thus, increased hyphal width on stiffer substrates could contribute to lower local ergosterol contents for 2 and 4 wt% agar substrates compared to the 1 wt% agar substrate due to a decrease in the hyphal cell wall-to-volume ratio. Since local growth analysis does not account for extensional fungal growth in the agar plate, it is reasonable to measure the highest ergosterol values in the softest substrate. This can be attributed to increased growth in the  $z$ -plane, as the mycelium encounters less resistance and grows more into the softer substrate. Hyphae apply turgor pressure to penetrate the substrate matrix, making softer substrates more susceptible to invasion.<sup>60,62</sup> In this study, we focused on how substrate stiffness affects overall biomass accumulation. We did not specifically investigate how substrate stiffness influences distinct stages of mycelial development, which could be explored in future studies.

Based on the results shown in Fig. 5, we can draw two key conclusions regarding the influence of the host material stiffness on mycelial growth. First, the extensive growth of mycelium (2D) is positively correlated with the host material's stiffness. Second, the mycelial biomass accumulation quantified *via* ergosterol (global growth) is negatively correlated with agar concentration.

### Limitations in strain generalizability

Beyond the specific experimental findings, a limitation of this study is the focus on a single fungal strain, which restricts the generalization of our findings. The use of ergosterol as a biomarker is applicable across fungal species; however, as our findings highlight, each strain requires an individual calibration curve relating ergosterol content to fungal biomass. The speed of hyphal extension can differ among Basidiomycete strains, which would impact the amount of ergosterol produced. With respect to growth dynamics, additional tests with a broader range of strains are necessary to evaluate the generalizability of the observed patterns. For example, while our previous work has shown similar trends in the effect of malt extract concentration among *Ganoderma* species,<sup>18</sup> the influence of substrate stiffness may vary more widely. Studies have shown that sensitivity to substrate stiffness is strain-dependent,<sup>60</sup> which could affect both hyphal penetration and



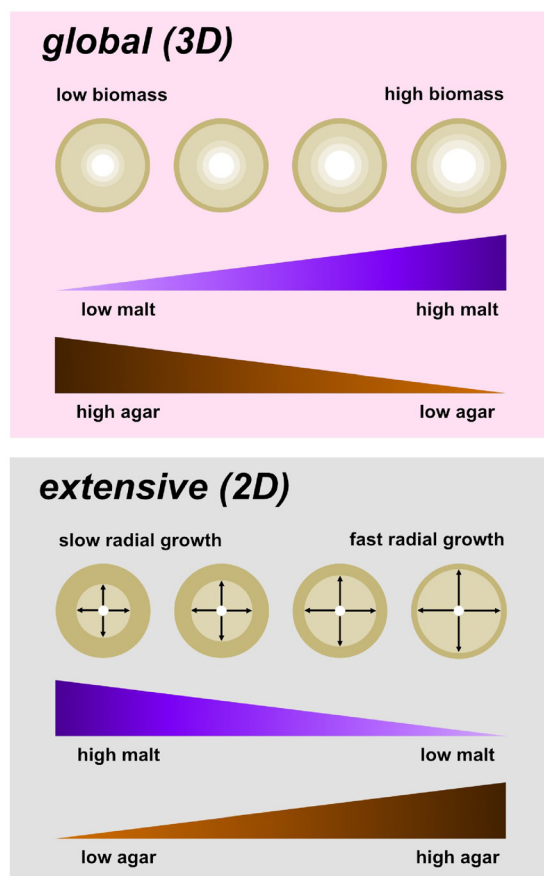


Fig. 6 Effect of increasing malt extract or agar concentration in the solid substrate on global biomass (3D) and extensive (2D) mycelial growth.

lateral growth. Nevertheless, the methodology developed here is broadly applicable, and future studies employing diverse strains will be essential to confirm its robustness and versatility.

## Conclusion

In conclusion, our findings establish ergosterol as a reliable biomarker for assessing fungal biomass, facilitating the investigation of 3D mycelial growth patterns based on directional growth within a sample. This represents an advance over traditional ergosterol assays, which primarily estimate bulk fungal biomass without resolving growth modes or spatial distribution. The quantification of ergosterol in solid-state fermentation provides a precise understanding of overall mycelial biomass accumulation, offering a robust framework to explore how different host material compositions influence mycelial growth dynamics. This is particularly important in contexts, where the substrate acts as a 3D host material, making it challenging to separate mycelial biomass for analysis. Our findings highlight that when using a standard substrate of 2 wt% malt extract and 2 wt% agar, extensive growth in the *x*-direction is the driving force for an increased global biomass accumulation, with local growth patterns only contributing a minor portion. The

correlation between faster extensive growth (2D) and increased global biomass (3D) does not always remain valid. Increasing nutrient density in the substrate through the addition of malt extract increases global biomass accumulation; however, this is accompanied by a reduction in radial (extensive) growth rate. Similarly, variations in substrate hardness by adapting the agar concentration in the substrate influence the growth dynamics: softer host materials facilitate increased global biomass accumulation while slowing radial growth, whereas increased substrate stiffness results in reduced global biomass accumulation, but promotes faster radial growth (Fig. 6). These insights advance our understanding of the complex host-material mycelium interaction during solid-state fermentation. Looking forward, these findings can inform the design and optimization of biotechnological processes that rely on fungal biomass, such as mycelium-based material production, bioremediation systems, and fungal bioconversion technologies. Future research should explore how ergosterol-based biomass assessment can be integrated into real-time monitoring frameworks, particularly in bioreactor and solid-state fermentation systems, enabling dynamic control of growth conditions for tailored biomass yields and material properties. Additionally, expanding this framework to different fungal species and diverse substrates will help generalize its applicability and deepen our understanding of fungus–substrate interactions in three-dimensional environments. Imaging-based approaches, such as confocal microscopy, could complement ergosterol quantification by providing spatially resolved validation of 3D growth patterns. Together, these advances will be directly relevant for scaling up to industrial applications, where robust, high-throughput monitoring tools are essential for the production of sustainable biomaterials and for enhancing the efficiency and reproducibility of large-scale fermentation processes.

## Author contributions

Natalie Nussbaum: conceptualization, data curation, formal analysis, investigation, methodology, project administration, validation, visualization, writing – original draft, review & editing. Laura Balmelli: data curation, formal analysis, investigation, methodology, validation, writing – review & editing. Nadja Steiger: investigation, methodology. Laura Nyström: resources, writing – review & editing. Peter Fischer: conceptualization, funding acquisition, project administration, resources, supervision, writing – review & editing. Patrick Rühls: conceptualization, funding acquisition, project administration, resources, supervision, writing – review & editing.

## Conflicts of interest

There are no conflicts to declare.

## Data availability

All data generated or analyzed during this study are included in this published article and its SI. See DOI: <https://doi.org/10.1039/d5ma00811e>.



No additional datasets were generated or analyzed during the current study, and no public repository deposition is required.

## Acknowledgements

NN, PF and PR acknowledge support for the research of this work from the Gebert R f Stiftung within the ‘Microbials: Direct Use of Micro-Organisms’ program (Project: GRS-095/20). The authors thank the Food Biochemistry Group at ETH for generously providing their expertise and access to their HPLC equipment and laboratory facilities. Special thanks are owed to Linda Destani and Samy Boulos for their valuable knowledge and support. We extend our sincere gratitude to MOGU Srl and Mycogenetics for providing the strains used in this study. Lastly, the authors thank Ciatta Wobill and Joseph D mpler for their helpful discussions and assistance.

## References

- 1 J. Luo, X. Chen, J. Crump, H. Zhou, D. G. Davies, G. Zhou, N. Zhang and C. Jin, *Constr. Build. Mater.*, 2018, **164**, 275–285.
- 2 M. E. Antinori, M. Contardi, G. Suarato, A. Armirotti, R. Bertorelli, G. Mancini, D. Debellis and A. Athanassiou, *Sci. Rep.*, 2021, **11**, 12630.
- 3 M. Jones, A. Gandia, S. John and A. Bismarck, *Nat. Sustainability*, 2020, **4**, 9–16.
- 4 A. Adamatzky, A. Nikolaidou, A. Gandia, A. Chiolerio and M. M. Dehshibi, *BioSystems*, 2021, **199**, 104304.
- 5 S. Gantenbein, E. Colucci, J. K ch, E. Trachsel, F. B. Coulter, P. A. R hs, K. Masania and A. R. Studart, *Nat. Mater.*, 2023, **22**, 128–134.
- 6 M. R. Binelli, P. A. R hs, G. Pisaturo, S. Leu, E. Trachsel and A. R. Studart, *Biomater. Adv.*, 2022, **141**, 213095.
- 7 E. Elsacker, M. Zhang and M. Dade-Robertson, *Adv. Funct. Mater.*, 2023, **33**, 2301875.
- 8 J. H. Teoh, E. Soh and H. Le Ferrand, *Int. J. Bioprint.*, 2024, **10**, 3939.
- 9 C. Wobill, P. Azzari, P. Fischer and P. A. R hs, *ACS Biomater. Sci. Eng.*, 2024, **10**, 6241–6249.
- 10 M. Jones, A. Mautner, S. Luenco, A. Bismarck and S. John, *Mater. Des.*, 2020, **187**, 108397.
- 11 S. Sivaprasad, S. K. Byju, C. Prajith, J. Shaju and C. R. Rejeesh, *Mater. Today: Proc.*, 2021, **47**, 5038–5044.
- 12 D. Saez, D. Grizmann, M. Trautz and A. Werner, *Biometrics*, 2022, **7**, 78.
- 13 E.  zdemir, N. Saeidi, A. Javadian, A. Rossi, N. Nolte, S. Ren, A. Dwan, I. Acosta, D. E. Hebel, J. Wurm and P. Eversmann, *Biomimetics*, 2022, **7**, 1–19.
- 14 M. Ruggeri, D. Miele, M. Contardi, B. Vigani, C. Boselli, A. Icaro Cornaglia, S. Rossi, G. Suarato, A. Athanassiou and G. Sandri, *Front. Bioeng. Biotechnol.*, 2023, **11**, 1–10.
- 15 A. Trinci, *Microbiology*, 1969, **57**, 11–24.
- 16 S. Hunter, R. McDougal, M. J. Clearwater, N. Williams and P. Scott, *J. Microbiol. Methods*, 2018, **154**, 33–39.
- 17 D. C novas, L. Studt, A. T. Marcos and J. Strauss, *Sci. Rep.*, 2017, **7**, 4289.
- 18 N. Nussbaum, T. von Wyl, A. Gandia, E. Romanens, P. A. R hs and P. Fischer, *Sci. Rep.*, 2023, **13**, 21051.
- 19 C. Scotti, C. Vergoignan, G. Feron and A. Durand, *Biochem. Eng. J.*, 2001, **7**, 1–5.
- 20 G. Vidal-Diez de Ulzurrun, J. M. Baetens, J. Van den Bulcke, C. Lopez-Molina, I. De Windt and B. De Baets, *Fungal Genet. Biol.*, 2015, **84**, 12–25.
- 21 L. De Ligne, G. Vidal-Diez de Ulzurrun, J. M. Baetens, J. Van den Bulcke, J. Van Acker and B. De Baets, *IMA Fungus*, 2019, **10**, 7.
- 22 M. Reeslev and A. Kjoller, *Appl. Environ. Microbiol.*, 1995, **61**, 4236–4239.
- 23 S. Steudler and T. Bley, *Filaments in Bioprocesses. Advances in Biochemical Engineering/Biotechnology*, Springer, 2015, vol. 149, pp. 223–252.
- 24 E. Favela-Torres, J. Cordova-L pez, M. Garc a-Rivero and M. Guti rrez-Rojas, *Process Biochem.*, 1998, **33**, 103–107.
- 25 L. Ooijkaas, J. Tramper and R. Buitelaar, *Enzyme Microb. Technol.*, 1998, **22**, 480–486.
- 26 M. Haneef, L. Ceseracciu, C. Canale, I. S. Bayer, J. A. Heredia-Guerrero and A. Athanassiou, *Sci. Rep.*, 2017, **7**, 41292.
- 27 H. A. W sten, M.-A. van Wetter, L. G. Lugones, H. C. van der Mei, H. J. Busscher and J. G. Wessels, *Curr. Biol.*, 1999, **9**, 85–88.
- 28 C. Schunke, S. P ggeler and D. E. Nordzieke, *Front. Microbiol.*, 2020, **11**, 1–10.
- 29 D. J. Barry, C. Chan and G. A. Williams, *J. Ind. Microbiol. Biotechnol.*, 2009, **36**, 787–800.
- 30 A. Groth, C. Schunke, E. J. Reschka, S. P ggeler and D. E. Nordzieke, *J. Fungi*, 2021, **7**, 580.
- 31 B. Guti rrez-Medina and A. V zquez-Villa, *Fungal Genet. Biol.*, 2021, **150**, 103549.
- 32 D. Zamir, O. Galsurker, N. Alkan and E. Eltzov, *Talanta*, 2020, **217**, 120994.
- 33 O. Radwan, M. C. Brothers, V. Coyle, M. E. Chapleau, R. R. Chapleau, S. S. Kim and O. N. Ruiz, *Biosens. Bioelectron.*, 2022, **211**, 114374.
- 34 R. Prasad, A. H. Shah and M. K. Rawal, *Advances in Experimental Medicine and Biology*, Springer, 2016, pp. 327–349.
- 35 M. O. Gessner, *Methods to Study Litter Decomposition: A Practical Guide*, Springer International Publishing, 2020, pp. 247–255.
- 36 M. O. Gessner and E. Chauvet, *Appl. Environ. Microbiol.*, 1993, **59**, 502–507.
- 37 S. Matcham, B. Jordan and D. Wood, *Appl. Microbiol. Biotechnol.*, 1985, **21**, 108–112.
- 38 H. Montgomery, C. Monreal, J. Young and K. Seifert, *Soil Biol. Biochem.*, 2000, **32**, 1207–1217.
- 39 A. Beni, E. Soki, K. Lajtha and I. Fekete, *J. Microbiol. Methods*, 2014, **103**, 124–130.
- 40 C. Mille-Lindblom, E. von Wachenfeldt and L. J. Tranvik, *J. Microbiol. Methods*, 2004, **59**, 253–262.
- 41 M. Brosed, J. Jabiol and M. O. Gessner, *Fungal Ecol.*, 2017, **29**, 96–102.



- 42 V. Gulis, K. A. Kuehn, L. N. Schoettle, D. Leach, J. P. Benstead and A. D. Rosemond, *ISME J.*, 2017, **11**, 2729–2739.
- 43 E. Baath, *Soil Biol. Biochem.*, 2001, **33**, 2011–2018.
- 44 K. Salazar Alekseyeva, B. Mähner, F. Berthiller, E. Breyer, G. J. Herndl and F. Baltar, *J. Fungi*, 2021, **7**, 690.
- 45 M. Bertasa, A. Dodero, M. Alloisio, S. Vicini, C. Riedo, A. Sansonetti, D. Scalarone and M. Castellano, *Eur. Polym. J.*, 2020, **123**, 109442.
- 46 E. G. Bligh and W. J. Dyer, *Can. J. Biochem. Physiol.*, 1959, **37**, 911–917.
- 47 L. Kolarič and P. Šimko, *J. Food Sci.*, 2020, **14**, 118–124.
- 48 M. A. Paulazo and A. O. Sodero, *PLoS One*, 2020, **15**, e0228170.
- 49 S. Marín, A. J. Ramos and V. Sanchis, *Int. J. Food Microbiol.*, 2005, **99**, 329–341.
- 50 H. Fujikawa, A. Kai and S. Morozumi, *J. Food Hyg. Soc. Jpn.*, 2004, **45**, 250–254.
- 51 A. Lo Grasso, A. Fort, F. F. Mahdizadeh, A. Magnani and C. Mocenni, *Math. Comput. Modell. Dyn. Syst.*, 2023, **29**, 169–185.
- 52 J. Feng, J.-S. Zhang, W. Jia, Y. Yang, F. Liu and C.-C. Lin, *Biotechnol. Bioprocess Eng.*, 2014, **19**, 727–732.
- 53 J. J. Classen, C. R. Engler, C. M. Kenerley and A. D. Whittaker, *J. Environ. Sci. Health, Part A: Toxic/Hazard. Subst. Environ. Eng.*, 2000, **35**, 465–488.
- 54 X. Tan, F. Chen, W. Hu, J. Guo and Y. Yang, *Int. Food Res. J.*, 2023, **30**, 709–722.
- 55 A. Ekblad, H. Wallander and T. Näsholm, *New Phytol.*, 1998, **138**, 143–149.
- 56 N. P. Money, *The Fungi*, Elsevier, 3rd edn, 2016, ch. 2, pp. 37–66.
- 57 J. Heitman, B. J. Howlett, P. W. Crous, E. H. Stukenbrock, T. Y. James and N. A. R. Gow, *The Fungal Kingdom*, American Society of Microbiology, 2017.
- 58 M. Nopharatana, T. Howes and D. Mitchell, *Biotechnol. Tech.*, 1998, **12**, 313–318.
- 59 M. Ghebremedhin, S. Seiffert and T. A. Vilgis, *Curr. Res. Food Sci.*, 2021, **4**, 436–448.
- 60 L. Yang, X. Hu and Z. Qin, *MRS Bull.*, 2024, **49**, 1205–1216.
- 61 E. C. Hotz, A. J. Bradshaw, C. Elliott, K. Carlson, B. T. Dentinger and S. E. Naleway, *J. Mater. Res. Technol.*, 2023, **24**, 7614–7623.
- 62 R. R. Lew, *Nat. Rev. Microbiol.*, 2011, **9**, 509–518.

